

# **Genotype Specific Pathogenicity of Hepatitis E Virus at the Human Maternal-Fetal Interface**

**Jordi Gouilly<sup>1</sup>, Qian Chen<sup>1</sup>, Johan Siewiera<sup>2</sup>, Géraldine Cartron<sup>3</sup>, Claude Levy<sup>4</sup>, Martine Dubois<sup>5</sup>, Reem Al-Daccak<sup>6</sup>, Jacques Izopet<sup>1,5</sup>, Nabila Jabrane-Ferrat<sup>1,\*</sup>, and Hicham El Costa<sup>1,5,\*</sup>**

<sup>1</sup>Centre of Pathophysiology Toulouse Purpan, INSERM U1043, CNRS UMR5282, Toulouse III University, 31024 Toulouse, France.

<sup>2</sup>University of California San Francisco, School of Medicine, Laboratory of Medicine, San Francisco, California, USA.

<sup>3</sup>Service de Gynécologie-Obstétrique, Hôpital Paule de Viguier, Centre Hospitalier Universitaire, 31059 Toulouse, France.

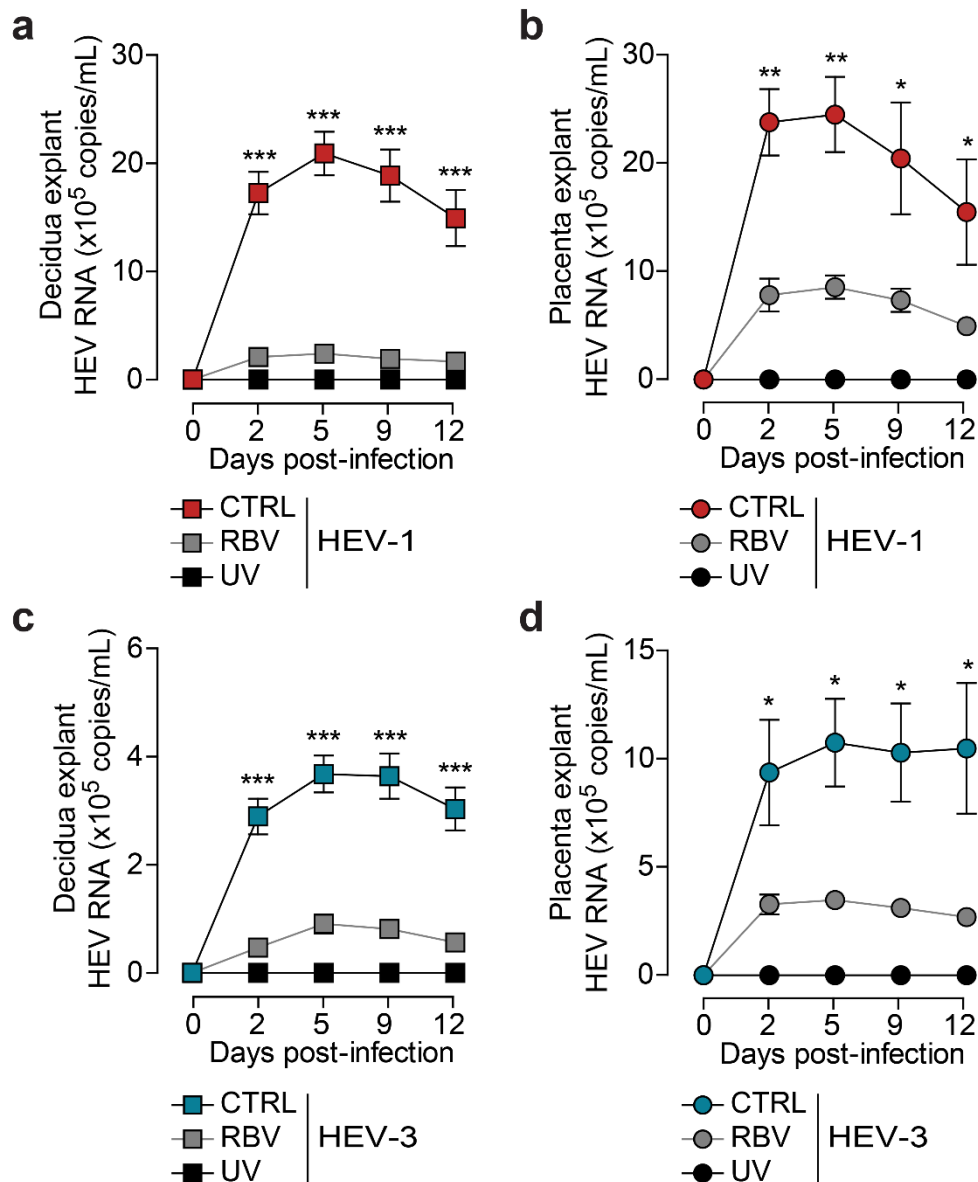
<sup>4</sup>Service de Gynécologie-Obstétrique, Clinique Sarrus-Teinturiers, 31300 Toulouse, France.

<sup>5</sup>Laboratoire de Virologie, Institute of Federative Biology, Centre Hospitalier Universitaire, 31059 Toulouse, France.

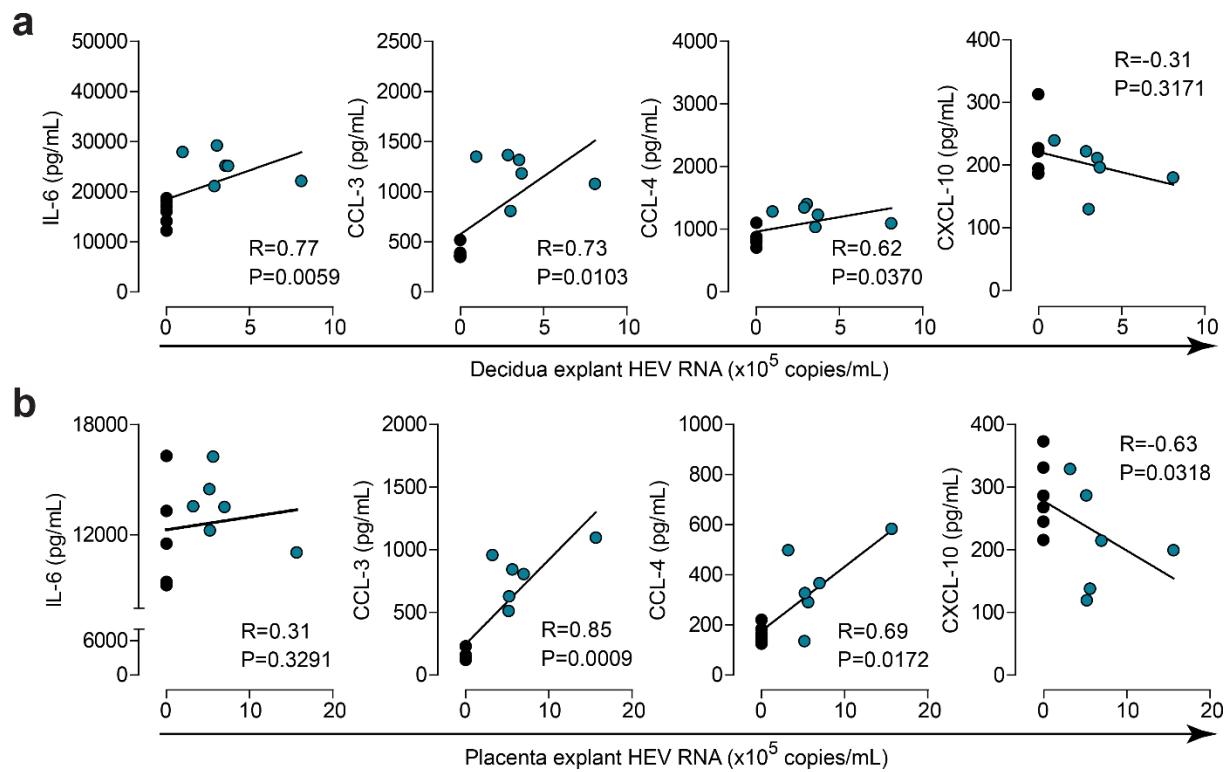
<sup>6</sup>INSERM UMRS976, Université Paris Diderot, Hôpital Saint-Louis, 75010 Paris, France.

\*These authors contributed equally and share senior authorship.

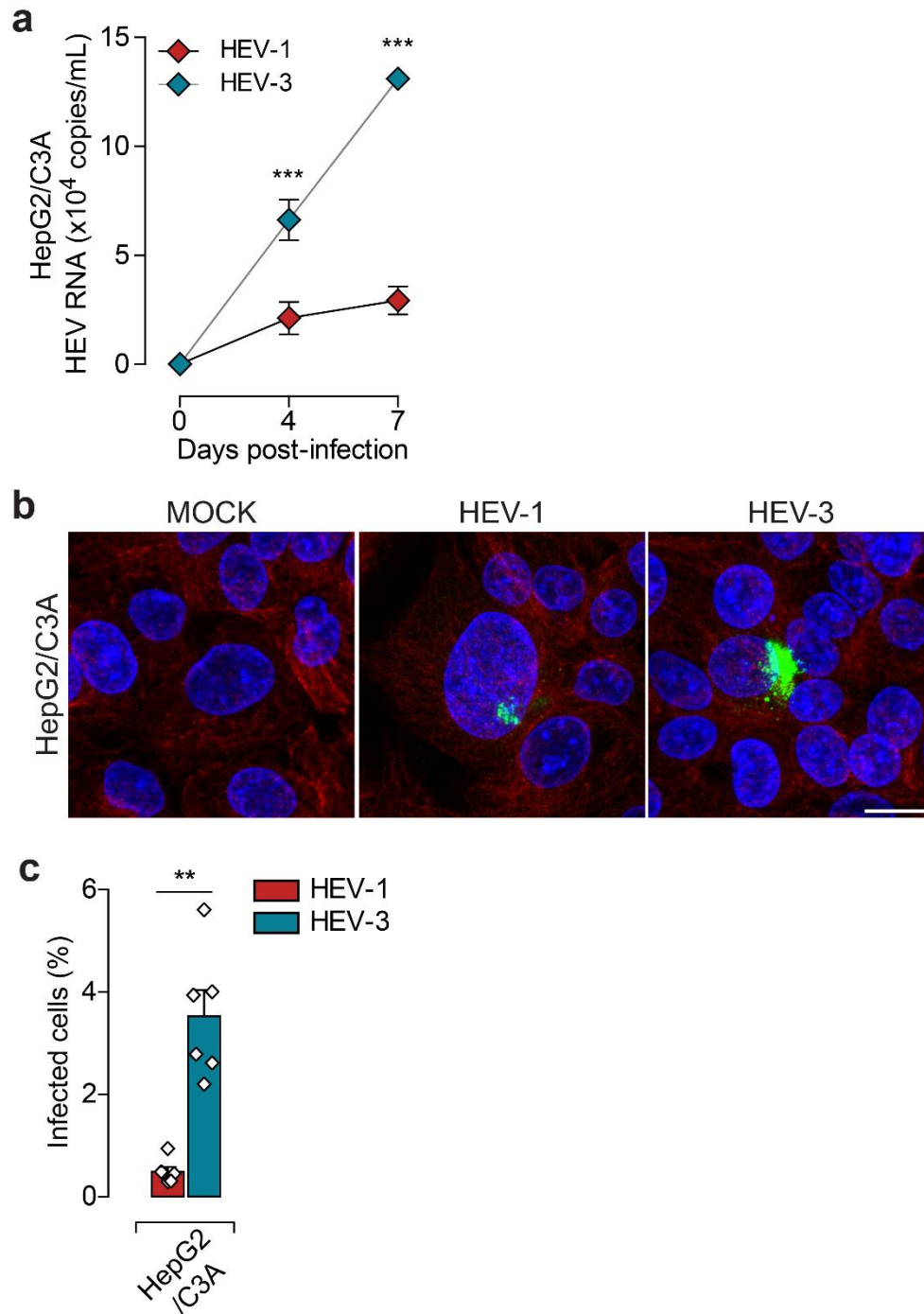
## Supplementary information



**Supplementary Figure 1. Ribavirin inhibits HEV-1 and HEV-3 replication in decidual and placental tissues.** Kinetics of HEV virus production from explants established from the decidua (**a,c**) and placenta (**b,d**), infected with HEV-1 (**a,b**; in red), or HEV-3 (**c,d**; in cyan). After infection, tissues were left untreated (CTRL) or treated with 50μM of ribavirin (RBV, in grey). UV-irradiated virions failed to infect decidual and placental explants (UV, in black). RNA levels were then measured in tissue culture supernatants by RT-qPCR. Data represent means values  $\pm$  S.E.M. of three independent donors. (\*) denotes a statistical comparison between CTRL- and RBV-treated infected tissues. \*  $P < 0.05$ ; \*\*  $P < 0.01$ ; \*\*\*  $P < 0.001$  by two-way ANOVA with Bonferroni post-hoc test.



**Supplementary Figure 2. HEV-3 infection of decidual and placental tissues skews their secretory function.** (a,b) Correlation between IL-6, CCL-3, CCL-4 or CXCL10 secretion and viral production in the decidua (a) and placenta (b) two days after HEV-3 infection. Black and cyan points represent mock-, and HEV-3-infected tissues respectively. The Spearman's rank correlation test P value and R coefficient are indicated in each graph. Data represent values of six independent donors.



**Supplementary Figure 3. HepG2/C3A cells are targets of HEV-3 and, to a lower extent, HEV-1 infection.** (a) Kinetic of viral RNA production in HepG2/C3A cell line, infected with either HEV-1 (in red) or HEV-3 (in cyan). Virus production was determined by RT-qPCR in culture supernatants. (b) Representative images of HepG2/C3A cells seven days after mock, HEV-1, or HEV-3 infection. Maximum intensity projections are shown. Staining indicates the ORF2 viral capsid protein (green),  $\alpha$ -tubulin (red), and nuclei (blue). Scale bar, 20 $\mu$ m. (d) Bar graph illustrating the percentage of infected HepG2/C3A cells seven days after HEV-1 (red) or HEV-3 (cyan) infection and determined by ORF2 staining. Data represent mean values  $\pm$  S.E.M. of three independent experiments. (\*) denotes a statistical comparison made between HEV-1 and HEV-3 infected cells. \*\* P<0.01; \*\*\* P<0.001 by two-way ANOVA with Bonferroni post-hoc test (a) and paired t-test (c).